Ultra-Low latency in Human-machine Interfacing using EMG Onset Detection and Pattern Recognition

by

Tushar Chopra

A thesis
presented to the University of Waterloo
in fulfilment of the
thesis requirement for the degree of
Master of Applied Science
in
System Design Engineering

Waterloo, Ontario, Canada, 2021

Author's Declaration

This research is composed of the material that I have written or co-authored: see the *Statement of Contributions* used throughout the thesis. This is a true copy of the dissertation, as agreed by my examiners, with any necessary final revisions.

Statement of Contributions

The publications and work that are associated with the work presented in this thesis:

1. Tushar Chopra, Jiayuan He and Ning Jiang "Ultra-Low Latency Detection of EMG Onset for Human-machine Interfacing" (Submitted to IEEE ICRA-2021).
2. Development of the product *"Impulse"* for a start-up named BrinkBionics, which is an EMG based glove that reduces a gamer's mouse click response delay.

Abstract

The research and development of advanced human-machine interfaces (HMI) have seen a significant surge during the last decade. These HMIs are gradually started to be integrated into our lives. Electromyography (EMG) is one of the types of signals which play vital roles in these HMIs. It is the electric manifestation of skeletal muscular activity. Traditionally, EMG processing is done by a sliding window-based paradigm, and the time windows used are usually in the order of several hundred ms long. This processing paradigm inevitably results in significant delay such that real-time detection of muscular onset with latency smaller than 10 ms is not possible. This long delay makes it difficult, if not impossible, for sEMG to be applied in many HMI applications where sufficiently short interaction delay is essential, such as virtual reality (VR), augmented reality (AR), and augmentation-on-demand exoskeleton.

This study investigated the viability of reducing PC mouse-click delay using surface Electromyography (sEMG) in Human-Machine Interface (HMI) applications. We examined three different real-time processing methods for sEMG onset detection along with a pattern recognition method for ultra-short latency. A PC mouse click protocol was used as the experimental setup, in which the participants were asked to perform both left and right mouse clicking tasks using their index and middle fingers. Surface EMG signals from the dorsal interossei muscles of the participants were acquired by dry sEMG electrodes. Teager–Kaiser Energy Operator (TKEO), root-mean-square (RMS), and a new onset detection method called Divergence Estimator (DE) were used to detect sEMG onset from one EMG channel. For the pattern recognition method a binary-class scenario was used: 'Click' class and 'No-Click' class.

The results showed that the proposed DE, combined with the binary classification approach, outperformed all other combinations of feature extraction methods and threshold detection or classification. The detection performance (F1-scores) of binary-classification were 0.87 and 0.88 for the left and right-click, respectively, which were significantly better

($p<0.05$) than all other onset-detection methods. Some detections were approximately 45 milliseconds ahead of the mouse button clicks of a top-of-the-line professional gaming mouse. Moreover, in different noise scenarios, our proposed method outperformed ($p<0.05$) TKEO and RMS for EMG onset-detection.

The outcomes in the current study demonstrated the possibility of using sEMG to establish an ultra-short latency human-in-the-loop human-robot interface, in which human motor intentions can be predicted in real-time before overt mechanical human movements occur.

Acknowledgments

I would like to thank my supervisor Professor Ning Jiang for providing me all the guidance, support, and patience throughout my Master's degree.

I would also like to express gratitude to my thesis readers, Professor John T.W. Yeow and Professor Clark Dickerson for their valuable feedback and suggestions.

I extend my gratitude to my co-authors Dr. Jiayuan He and Prof. Ning Jiang supported me in data collection, writing papers, and the research activities. I deeply thank all the participants who experimented in this study.

I would like to mention and thank the financial assistance of the University of Waterloo, Canada's (NSERC) Natural Sciences and Engineering Research Council of Canada.

I would like to thank my mother, Mrs. Shakuntala Chopra, father Mr. Kamal Kumar, and my three sisters, Meenakshi Chopra, Tanushri Chopra, and Jaya Chopra for their relentless love and encouragement, which helped me to pursue my Master's degree.

Dedication

To my beloved parents and three sisters.

Table of Contents

List of Figures

List of Tables

Chapter 1

Introduction and Background

1.1 Human-Machine Interaction

1.1.1 Overview

Human-Machine Interaction (HMI) implies communicating or transmitting information between a person and machine through an interface. Other common names are Human-Machine Interface and Man-Machine Interface; both refer to the same definition. In HMI, the machine can be a computer (known as Human-Computer Interaction) or any electrical or mechanical device, or even a virtual reality agent. A wide range of HMI devices is used currently in entertainment, machinery, and medical practices. Furthermore, in the last two decades, bio-signals-based technologies such as Brain-Computer Interface (BCI) and exoskeletons are gaining popularity in research studies due to commercial and medical applications, respectively.

1.1.2 Types

HMI can be broadly categorized into five categories [4]; each has a unique means to communicate and user interaction.

- **Optics**

  In Optics-based HMI, the primary hardware used are cameras, lasers, and LEDs. The cameras are used for computer vision, and a laser-led based system is used for distance calculation. Both work in conjunction with applications like robotics, self-driving cars [5], controlling wheelchairs from head gestures [6], giving inputs to the computer using eye-tracking [7], and more. Most of the applications are based on computer vision, such as object detection and detecting criminal or suicidal intentions from body language [8]. However, applications in HMI rely intensely on image recognition and motion tracking.

Figure 1.2: Type of HMI. Acoustic and Optics in the first two; Bionics in the centre; Motion and Touch in the last two respectively. [4].

- **Bionics**

  Bionics involves the collaboration of robotic, biological, and computer systems that operate together to trigger an action. This is typically achieved using bio-signals, which are captured using conductive electrodes. Different types of bio-signals that can be used to build the HMI system are Electroencephalography (EEG), Electromyography (EMG), Electrocardiography (ECG) signals, which are used to study brain, muscle, and heart activities, respectively.

- **Acoustic**

  Acoustic HMI relies on sound-based interaction with the system. Speech recognition and Text-to-Speech systems are the backbones of this type of HMI, where a specific set of words or text acts as a trigger to control a device. The system relies heavily on machine learning research, and the recent developments in deep learning and word vectors have drastically improved these systems. Some of the applications are voice-controlled appliances and wheelchairs [9], as well as voice-enabled music & entertainment controls in cars [10], home and mobile devices.

- **Motion**

  This type of HMI utilizes motion-based interaction with users. Usually, a predefined path of motion acts as a trigger in the device. Accelerometer and gyroscope are the typical technologies used in conjunction with other hardware such as mobile, virtual reality (VR), augmented reality (AR), and more. Some of the applications are teleoperation of robots [11], head rotations [12], driving a wheelchair [13].

- **Tactile**

  Tactile HMI requires physical touch to something by users, which is considered as input to the system. Mouse and keyboards are examples of tacile HMI. The most popular technology of tactile HMI is touch screens, which we used in our mobile, tablet, and laptops. Recently, a pressure-based toggling mechanism of buttons is used in mobile devices instead of the button's physical press. One application in medical practice is haptic feedback based surgical procedures [4].

1.1.3 EMG based HMI

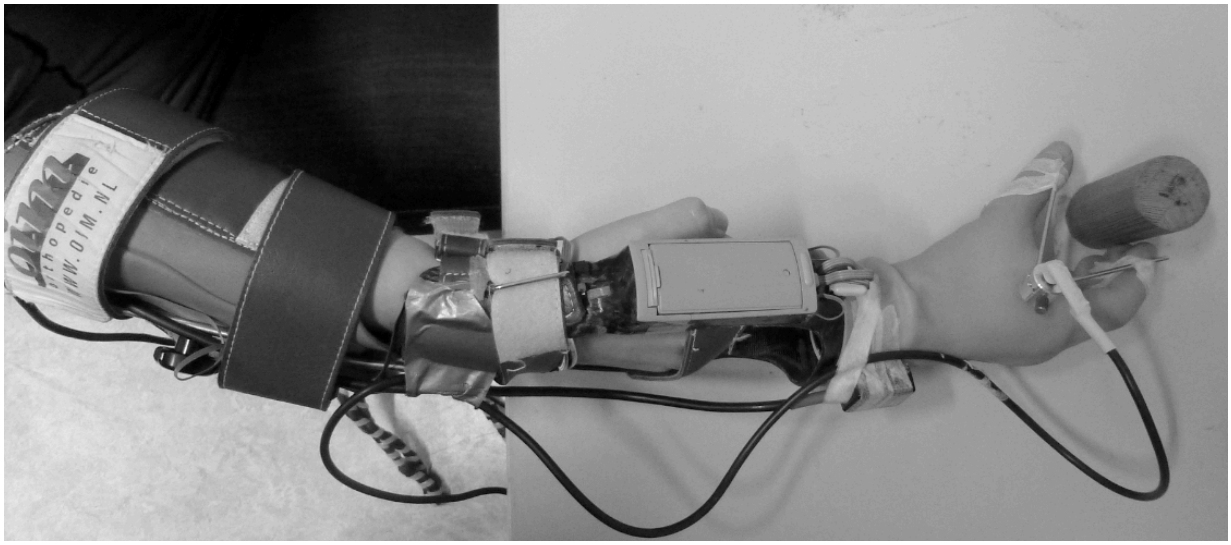

Figure 1.2: A EMG based controller for a video game; A myoelectric hand connected to participant's hand with an open cast [3].

A sub-category of the bionic HMI is one that utilizes EMG, which is the recording of the electrical activity of muscle recruitment. Compare to EEG, which is the recording of cortical neuron's electric activities and is usually in the range of microvolts, EMG is usually in millivolts, requires less sophisticated amplification instrumentation, and is less susceptible to various noise and artifacts. Several HMI applications rely on EMG, for instance, full-body exoskeleton to increase user strength [14], gesture recognition [15], motionless gestures [16], and myoelectric control [17].

Furthermore, EMG-based HMI in gaming is also used in rehabilitation [18] and for user engagement and participation. Previous studies used EMG to measure engagement in the Levee Patroller game training [19], in myo-gaming [3], or EMG controlled game to test improvement in prosthesis control.

1.1.4 Ultra-Low Latency

Low latency refers to a computer process that is fast enough to operate on a large volume of data with a small delay [20]. Moreover, when the processing delay is less than one millisecond, the system is considered ultra-low latency [21]. The ultra-low latency system's performance is very crucial in time-critical real-time applications. The acceptable processing delay in HMI devices varies based on the type of HMI and is subjective to each application. In surface EMG based bionics, typically hundreds of milliseconds of EMG data is required to make any prediction for an outcome. Multiple studies [22] try to reduce this delay in detecting EMG onsets. In a previous study [23], the authors show myoelectric control performance based on different window sizes and majority voting, which further delays the classification process. They stated the performance of pattern recognition is directly proportional to the window length.

1.2 Electromyography

1.2.1 Overview

Electromyography (EMG) is a method to record the electric manifestation of skeletal muscular activity. The information is captured using electrodes. The torque applied to the skeletal system joints due to muscle contraction leads to movement in the body. Muscles are composed of fibers that are innervated alpha motor neurons, which receive efferent neural drive descending from the central nervous system. A motor unit is made of motor neuron and all the muscle fibres which the neuron innervates. Each motor neuron controls a varying number of muscle fibers depending on different muscle types [24]. This number is called the *innveration* ratio. Motor neuron depolarization propagates as a wave through axons from the spinal cord to muscle fibres to activate a motor unit. The propagating depolarization of the neuronal membrane can be recorded by

electrodes placed in the vicinity of the membrane, and such activity is called a motor neuron action potential (MUAP). When the MUAP reaches the neuromuscular junction (NMJ), special neurotransmitters are released from the axon to the muscle fibre membrane, which depolarizes the muscle fibers. And such fibre depolarization would, in turn, propagate from the NMJ, along with the fibre, toward the two tendons, to which the fibres are attached. This propagating depolarization can also be detected by electrodes place in its vicinity and is called muscle fibre action potential. The collective muscle fibre actional potentials from the same motor unit often appear to be a single action potential because all fibres within the unit would be activated simultaneously. And this 'collective' action potential is often called the motor unit action potential. One motor unit action potential is often referred to as a 'firing' of a motor unit. The frequency of motor unit 'firing', or the firing rate ranges from 4-6 Hz (firings per second) to approximately 30-40 Hz. The above is a brief description of the electric process of muscular activation.

A mechanical process of muscular activation occurs simultaneously with this electric process. Upon the membrane depolarization, muscle fibres would shorten, resulting in mechanical contraction. The amount of contractile tension generated by the fibres differs among different types of muscle fibres. Furthermore, the overall contractile tension generated by a muscular contraction further depends on factors, such as how many motor units being activated [25]. The motor unit action potential, being an electromagnetic signal, can be detected at the skin surface, usually by Ag/Ag-Cl electrodes with conducting gel. The gel helps to reduce impedance between the skin and electrode. [26]. For long-duration applications, a gel electrode system is not preferred; instead, dry electrodes made of a material such as stainless steel or conductive ceramics are used. Dry electrodes often have higher noise levels due to higher electrode-skin impedance.

In addition to the above described non-invasive measurement of EMG, also known as surface EMG (sEMG), EMG can also be measured by invasive electrodes, such as needles or fine wires that are trans-cutaneously inserted into the muscle under investigation. This latter method is called intramuscular EMG. Although intramuscular EMG collectes muscle activity of individual muscle fibers, sEMG is more frequently used in disciplines outside neurophysiology, where these invasive methods are not practical due to problems such as electrode insertion, infection, and subject compliance. The sEMG signal contains two types of information, Time-Domain, and

Frequency-Domain, which depend upon intensity and duration of muscle contraction, electrode-amplifier configuration, skin-electrode contact quality, and placement of electrode with respect to muscle [27].

There are multiple sources of noise while acquiring EMG data, such as relative displacement between the recording electrode and the muscles under investigation, the movement of the electrode with respect to the skin, electromagnetic interferences due to power line, etc. This noise degrades the performance of the system and needed to be rectified before any processing. Multiple methods can be used to rectify these problems, such as filtering techniques like bandpass and stop, high and low pass filters. Noise such as power line noise and motion artifact can be largely removed with these techniques.

1.2.2 Onset Detection

Onset detection in sEMG refers to defining the exact point in time when activity begins. Various sEMG applications use it to perform a task based on the starting and ending of the muscle activity. In literature, several onset detection methods were previously used that includes threshold-based decision or visual examination [28]. Later TKEO introduced in [29] became the most widely used onset detection method in sEMG [30]. Authors [31] showed the efficacy of TKEO in improving signal-to-noise ratio (SNR) of surface EMG and reduced false onset detection. Numerous studies [30] [32] have used it either as a pre-processing step before feature extraction or as a decision-making method.

The major superiority of the nonlinear TKEO over other onset detection methods is that only three samples are required to operate, compared to other methods that require a larger amount of data. This helps in detecting the instantaneous change in the signal, which corresponds to the high-frequency information. Furthermore, the application of TKEO was also extended to identify sudden spikes or abrupt signal changes in bio-signals [33]. The TKE-Operator ψ is defined as:

$$\psi[x_{(n)}] = x_{(n)}^2 - x_{(n-1)} \cdot x_{(n+1)} \tag{1.1}$$

where $x(n)$ represents the EMG signal as a time series. For onset detection, a threshold is chosen as γ times the standard deviation of the base signal. The value of γ is specific to each dataset and

need to be determined. An onset or offset is considered when *n* consecutive samples are above or below the threshold, respectively.

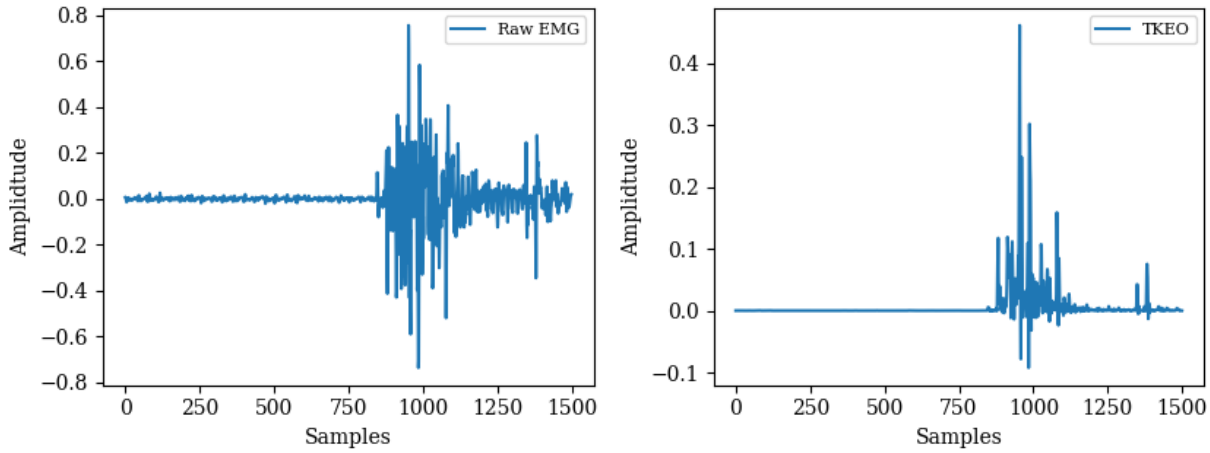

Figure 1.3: Effect of TKEO on raw EMG. A. Raw EMG of the muscle activity of a mouse click; B. Signal output after applying TKEO.

In addition to TKEO, studies [30] have also used Root Mean Square (RMS) value for EMG onset detection. The same threshold-based detection method can be applied to RMS. However, the authors of [30] reported this method was not feasible in the presence of significant noise in sEMG signals. In this study, the performances of both TKEO and RMS are investigated, and the results are reported in section 3.1. The equation of RMS is defined below.

$$Root\ Mean\ Square = \sqrt{\frac{1}{N}\sum_{i=1}^{N}(x_i)^2} \tag{2.2}$$

1.2.3 EMG based Pattern Recognition

Pattern recognition involves extracting knowledge and statistical information from the data to develop classification or regression capacity. It is a multi-stage process. The significant limitation of pattern recognition in EMG signals is low classification capacity due to high noise in the acquired data.

Feature extraction is the most critical stage in EMG based pattern recognition and there are several existing techniques available [34]. Most studies used time, frequency, and spatial domain features from the acquired data. Typically, time and spatial domain features are computationally simple and work well in real-time. In contrast, frequency-domain features require a bigger amount of data to extract information and thus increase processing time. Generally, pattern recognition based on frequency domain features performs better than time-domain features. Some common time-domain features are reported below.

- **Integrated EMG**

  It is the sum of absolute values of the signal's amplitude in the time-domain. This is typically used in onset detection in case of muscle contraction to control rehabilitation and assistive device.

$$Integrated\ EMG = \sum_{n=1}^{N} |x_n| \tag{3.3}$$

- **Mean Absolute Value**

  Followed by rectification, it is window based moving average of absolute values of the surface EMG signal. It is a popular feature in EMG pattern recognition applications, typically used in myoelectric control.

$$MAV = \frac{1}{N}\sum_{n=1}^{N} |x_n| \tag{4.4}$$

- **Variance of EMG**

  This feature extracts the power of the signal as a feature. It is the square of the standard deviation of the signal with a mean equal to zero in the case of surface EMG.

$$VAR = \frac{1}{N-1}\sum_{n=1}^{N} x_n^2 \tag{5.5}$$

- **Waveform Length**

  It is the additive length of signal in a fixed window size; in other words, the absolute sum of the difference of amplitudes in consecutive samples. Waveform length is associate with a feature that captures some frequency information from the time-domain itself.

$$WL = \sum_{n=1}^{N-1} |x_{n+1} - x_n| \tag{6.6}$$

- **Zero-Crossing**

  The number of times a signal crosses the y-axis at y equal to zero in a specific window size known as zero-crossings. The rationale is, high-frequency signals will have more zero-crossings than low-frequency signals. It can be used in the onset detection problem along with a threshold, but traditionally it is considered as a feature in the classification process.

$$ZC = \sum_{n=1}^{N-1} \begin{cases} 1, & \text{if } x_n \cdot x_{n+1} \geq threshold \\ 0, & \text{otherwise} \end{cases} \tag{7.7}$$

- **Slope Sign Change**

  It captures similar information as zero-crossing, but it calculates how many times, slope changes between positive and negative in consecutive samples. Typically, studies have used either zero crossings or slope sign change, as a feature in pattern recognition.

$$SSC = \sum_{n=2}^{N-1} f\{(x_n - x_{n-1}) \cdot (x_n - x_{n+1})\}$$
$$f(x) = \begin{cases} 1, & \text{if } x \geq threshold \\ 0, & \text{otherwise} \end{cases} \tag{8.8}$$

- **Willison Amplitude (WAMP)**

  Motivated from the previous two, Willison amplitude computes how many times differences in two consecutive samples' amplitudes exceeds the predefined threshold.

$$WAMP = \sum_{n=1}^{N-1} f(|x_n - x_{n-1}|)$$

$$f(x) = \begin{cases} 1, & \text{if } x \geq threshold \\ 0, & \text{otherwise} \end{cases} \tag{9.9}$$

Other features like the histogram of EMG, Root Mean Square, MAV-Slope, and more are also used in the EMG feature extraction process. These are generally applied in muscle onset detection and the multi-class classification process. The study [23] shows the efficacy of time-domain features in multi-function myoelectric control applications; the authors used four time-domain features collectively applied to linear discriminant analysis (LDA) classifier and obtained results with less than five percent error.

Frequency domain features are also used in the multi-class classification process and are often considered more robust than time-domain features. Typical applications are fatigue detection in muscles [35] and neurological deformity. Mean frequency and median frequency are the traditional features that are used in EMG. In [17], the authors utilized power in multiple pre-selected frequency sub-bands along with other features to linear regression, which proved superior to traditional time-domain features. Frequency domain features are extracted using the power spectrum and Fourier transformations, which require a significant amount of data to process, hence not recommended for real-time systems. Other methods such as the Autoregressive model also exist, which relies on the assumption that a system's current behavior relies on past behavior of the system in time, which is described as:

- **Autoregressive Coefficient (AR)**

$$x_n = -\sum_{n=1}^{p} a_i \cdot x_{n-i} + w_n \tag{10.10}$$

Here, x_n, p, a_i, w_n are the current sample of the signal, order of autoregressive model, autoregressive coefficients, and white noise, respectively. AR is used in fatigue

applications [36], where authors have used the fourth-order, generally, an order between one to ten is seen for sEMG studies.

1.2.4 Hand Muscle Anatomy

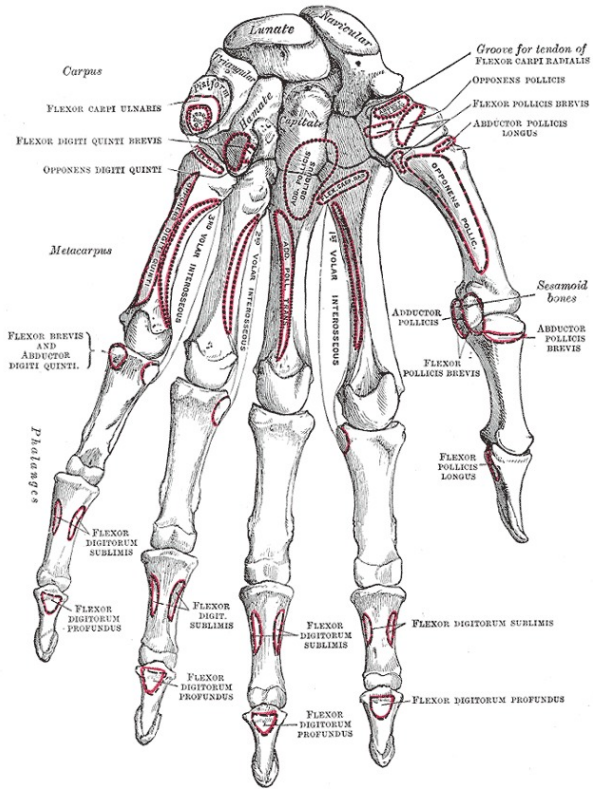

Figure 1.4: Hand Muscle Anatomy [2].

Muscles connected to the human hand skeleton are skeletal muscles. These muscles are responsible for hand movements and the control of individual fingers [37]. If recorded properly, electric manifestation in these muscles can be detected at the skin surface, which is surface EMG [38]. There are two types of muscles controlling the functions of the hand, intrinsic and extrinsic.

Extrinsic hand muscles are responsible for gross movements of hands like hand close and hand stretch. These muscles are situated between the anterior and posterior sections of the forearm and are comprised of *extensors* and *long flexors*. Finger muscles include two *long flexors* and are present in the forearm. The superficial flexor is connected to the *middle-phalanx* and the *deep flexor* to the *distal phalanx*. The functioning of finger bending relies on these *flexors*. The thumb muscles

consist of two small and long *flexors* in the *thenar* muscle group. This group also includes other muscles like the *opponens* and *abductor brevis* muscle, responsible for thumb movement and grasping of objects.

Intrinsic hand muscles are smaller and are present distal to the wrist joint. Subtle motor movements of the finger are controlled by these intrinsic muscles. These muscles are comprised of *thenar* and *hypothernar*, the *interossei*, and the *lumbrical* muscles [2]. Both *thenar* and *hypothenar* muscles consist of three muscles located at the bottom of the thumb and the little finger, respectively.

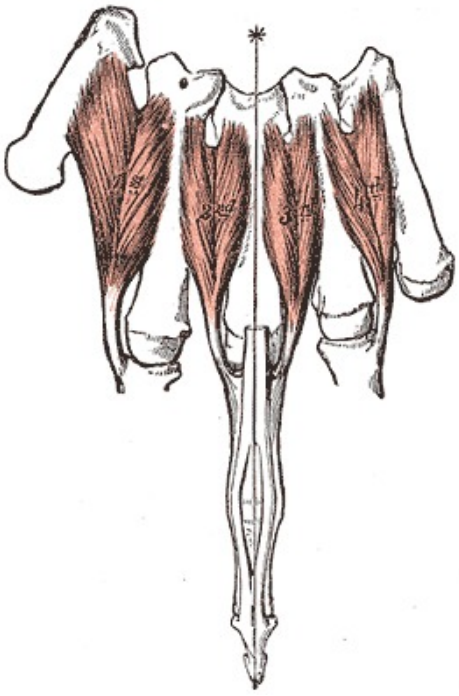

Figure 1.5: First, second, third and fourth dorsal interossei muscles of the hand [**1**].

The *interossei* have four *dorsal* and three *palmar* muscles. Furthermore, *lumbrical* muscles comprise four muscles, which all act on *metacarpophalangeal*, connected to their respective places.

1.2.4.1 Dorsal Interossei

There are four *dorsal interossei* in the hand (Figure 1.5), which exist in between the *metacarpals* of the hand [1, 39]. The shape of these muscles is bipennate and they are responsible for the spread of the index, middle, and ring finger. Their function also includes *flexion* of the same

fingers at *metacarpophalangeal* joints. Our study is focused on investigating sEMG from first and third *dorsal interossei* to detect the mouse click muscle movement before the physical mouse click. Muscular contractions of these small muscles are sufficient to generate a mouse click. Consequently, the associated sEMG activity is small in magnitude, which makes click detection a challenging problem. This study examined the possibility of click detection and investigated the detection delay of the sEMG onset.

1.3 Pattern Recognition

1.3.1 Overview

Pattern recognition is the process of identifying characteristics of known data that can be utilized to perform classification or regression to unseen data. Often EMG applications follow a series of steps for classification, which involves filtering and pre-processing, feature extraction and reduction, model training, followed by real-time or off-line classification [40].

The process starts with acquiring the EMG signal from the participant in a study followed by initial pre-processing steps of amplifying, rectification, or filtering. Previous studies have used an infinite impulse response (IIR) Butterworth filter for filtering EMG [17]. IIR filters are recursive in nature; they take current and previous inputs to generate the output. A low pass filter is used to remove high-frequency noise, and a high pass filter is used to remove low-frequency motion artifacts; studies have also used a combination of both known as a band-pass filter.

The feature extraction is a vital part of pattern recognition, affecting its performance. There are multiple time domain and frequency domain features extracted from surface EMG to improve the robustness of the system, refer to section 1.2.3. The time-domain features are the most widely used in EMG applications due to their simplicity, making them adequate for real-time processing. Different time-domain features represent specific information of the signal, which is being used by the classifier to build the model.

The next step consists of feature reduction or dimensionality reduction in the case of redundant information in extracted features and to avoid the *curse of dimensionality*. Various

means to achieve this are principal component analysis (PCA), auto-encoders, high correlation filter, backward feature elimination, low variance filter, and more. The most widely used method is PCA. A good dimensionality reduction stage facilitates the model learning process, which improves the system's classification performance [41].

The last stage consists of model training in the reduced feature space that represents patterns for different motions. Generally, supervised learning is used to train classifiers. In this case, the classifier uses known data to develop classification intuition. The classifier's performance is then evaluated on novel data, and accuracy obtained using predicted and true labels. The process is then repeated with different classification algorithms followed by hyper-parameter tuning to improve the robustness; then the best algorithm is chosen for further system development [42].

1.3.2 Classification Algorithms

The selection of best-suited features and classification algorithm constitutes a suitable pattern recognition method. Various classifiers are standard in practice for surface EMG studies such as Linear Discriminant Analysis (LDA), Logistic Regression, K-Nearest Neighbors (KNN), Support Vector Machines (SVM), Artificial Neural Networks, Naive Bayes [43] and more. LDA, which is the simplest and most straightforward in implementation, is the first preference as classifiers in various scientific studies [23, 41]. It can classify different muscle activations and the onsets of multiple intended movements [44]. The permanence of a classifier is measured by its classification accuracy, which is calculated by how many times a system correctly detects the respective movements. The performance of LDA and SVM classifiers are found very similar in the prosthetic control. Below are the details of some common algorithms.

- **Linear Discriminant Analysis (LDA)**

  In dimensionality reduction, LDA works as an algorithm to reduce the number of dimensions using supervised learning. This is done by transforming higher dimension features to a lower dimension feature set. In total, *C-1* dimensions are being selected, with *C* being the total number of classes.

$$y = w^T \cdot x + w_0 \tag{11.11}$$

The objective is to find the projection *y*, with *x* and *w* being the input data and projection vector, respectively. Similar to Fisher linear discriminant, LDA is also being used as a classifier in a pattern recognition problem. It has three main steps. First, inter-class separability is computed using means of different classes; the second intra-class variance is computed. Third, a lower dimension space is selected, which maximizes inter-class distance and minimized the intra-class spread of data.

$$J(w) = \frac{|\overline{\mu_1} - \overline{\mu_2}|}{\overline{s_1}^2 + \overline{s_2}^2} \tag{12.12}$$

where, $\overline{\mu_1}$ and $\overline{\mu_2}$ are the means of two classes, and $\overline{s_1}$ and $\overline{s_2}$ are the variance of each class from its own data points. Next, $J(w)$ needs to be maximized $argmax\, J(w)$ which can be transformed as

$$J(w) = \frac{w^T S_B w}{w^T S_W w} \tag{13.13}$$

matrix S_B and S_w are between class and with-in class scatter, respectively. The separability between the classes can be maximized with an appropriate w that maximizes $J(w)$

$$argmax_w J(w) = \underset{w}{argmax} \frac{w^T S_B w}{w^T S_W w} \tag{14.14}$$

Fisher first proposed linear discriminant analysis, and it is a linear classifier that works well on linear or gaussian data. For nonlinear data, Quadratic discriminant analysis (QDA) is preferred, which projects data into higher dimensional space to increase class separability.

- **Logistic Regression**

  In pattern recognition, logistic regression is most widely used to solve a binary classification problem. Not to confuse with linear regression, which is used to predict continuous values, logistic regression takes the output and passes it to a sigmoid function, which returns a probability value based on which the respective class is assigned. The core of the algorithm is sigmoid function *S(z)*, whose output varies between 0 and 1.

$$S(z) = \frac{1}{1 + e^{-z}} \tag{15.15}$$

  where *z* is the input. Typically the threshold for decision boundary is 0.5; if the probability is greater than the threshold, it belongs to a positive class; otherwise, it belongs to a negative class. Some of the applications are neuromuscular disorder classification and prosthetic hand [45].

Although multiple pattern recognition techniques are used in practice such as Random Forest, Quadratic Discriminant Analysis, and more, in EMG studies, LDA and SVM seem the first choice for EMG analysis.

1.3.3 EMG Pattern Recognition Limitations

In sEMG applications, classification is done using a sliding window-based system, and the time windows used are usually in the order of several hundred milliseconds long. This induces delay and makes the application challenging to work in time-critical real-time environments. Another limitation of EMG based pattern recognition is some studies have come up with proportionality estimator schemes [46, 47] which is not as intuitive as the regression-based control. Moreover, most prosthetics pattern recognition techniques can provide only one degree of freedom, which is an unusual experience and a difficult task for an amputee to control. In a prosthetic arm, multiple degrees of freedom and simultaneous control is expected to be fully functional and comparable to a natural human limb. Some studies [48] have also explored the usage of non-linearities of artificial neural networks to estimate wrist kinematics using surface EMG.

1.4 Thesis Outline

The principal objective of this study is to investigate the possibility of low latency HMI using surface EMG. Two key approaches, onset-detection and pattern recognition, were examined to achieve this. Moreover, instead of traditional window-based classification in bio-signals, sample by sample classification was investigated. Also, the relation between low-latency detection performance and increasing window size in surface EMG was explored.

The rest of the dissertation is structured as follows: Chapter 2 contains the details of experiment design, data collection, analysis, and the methods used. It also describes the novel feature extraction algorithm along with the pattern recognition method used in this study. Chapter 3 explains the results and analysis of the experiments performed. For both, proposed new features and pattern recognition method, the results are discussed in the context of mouse click detection performance and average detection latency. Chapter 4 discuss the results, real-time implications, limitations of the study, and its significance, followed by the conclusion and future work in Chapter 5.

Chapter 2

Methodology

This chapter explains the experiment setup, terminologies, methods, and performance metrics used in our study.

2.1 Participants

The study consisted of twenty healthy participants (seven females and thirteen males) with an age range from 19-30 years. Participants were allowed to ask any questions and withdraw from the experiment at any point of the study. The study and experiment were approved by the Office of Research Ethics of the University of Waterloo (ORE 23061). Consequently, a consent form was signed for the same by each participant at the beginning of the experiment.

2.2 Instrumentation

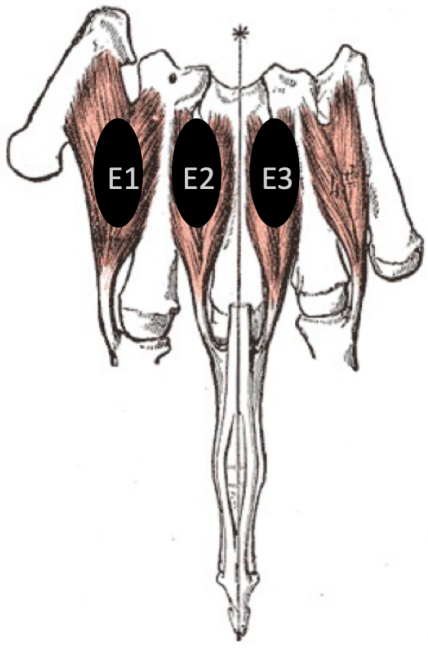

Figure 2.1: Placement of three bipolar dry electrodes (E1, E2, E3) over first (E1), second (E2), and third (E3) dorsal interossei muscles.

The instrumentation consisted of acquiring surface EMG signals using a custom-made amplifier with three bi-polar dry electrodes (Danyang Incorporation, China) and a micro-controller (STM-32). The three dry electrodes were positioned on the dorsal side of the hand, refer to Figure 2.1, over the first, second, and third dorsal interossei muscles with the help of an adjustable elastic strap-on. 2048 Hz sampling rate was used with the analog filter (Butterworth 5th order band-pass filter; 10-500 Hz), which was used before digitizing sEMG data to 12-bit precision. An alcohol swap was used to clean the skin before electrode placement. A desktop application was developed in Electron/Node JS for UI and C/C++ for signal acquisition, processing, model development, and saving results. For mouse click timings, Microsoft Win32 API written in C was used simultaneously to get exact click timings and status.

2.3 Experiment Protocol

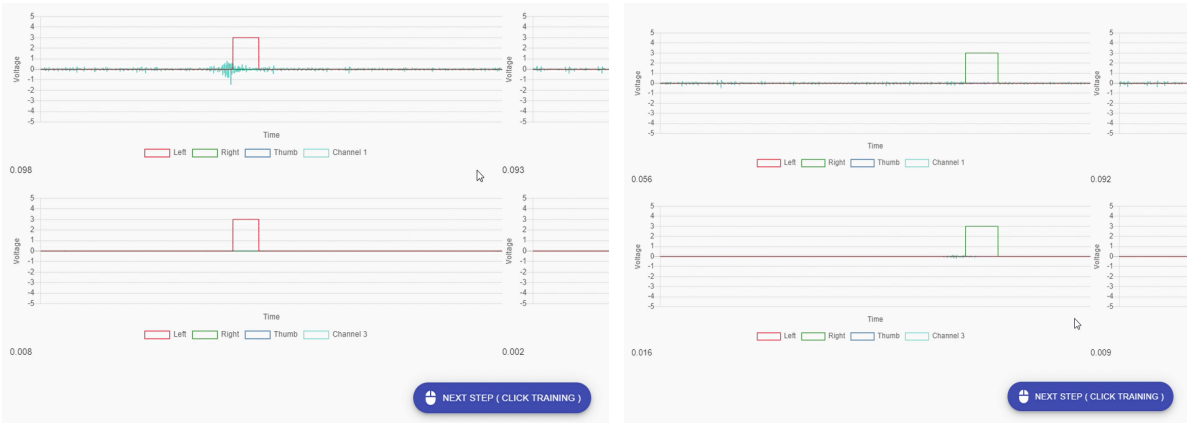

Figure 2.2: *'Calibration'* phase; Participants can see their real time muscle activity and mouse click timings. The Red ones are 'LEFT' clicks and green ones are 'RIGHT' clicks. First and second row shows the muscle activity of first and third channels of the glove, respectively.

The experimental protocol consisted of three phases: the *'calibration'* phase, the *'training'* phase, and the *'real-time running'* phase, completed in this order by all participants. Participants could see their visual real-time sEMG activity and their mouse clicks (LEFT & RIGHT) information in all three phases. Moreover, for the *real-time running* phase, the detection algorithm's outcome (detections of mouse clicks) could also be seen visually, along with the lead time of each click. After the electrode setup, the *'calibration'* phase would begin, during which the participants were given time between 15-20 minutes to get used to the setup. He/she could

move their mouse, perform clicks anywhere on the screen, and see his/her real-time sEMG and clicks information (see Figure 2.1). For some participants, the EMG activity of one of the click types (LEFT or RIGHT) was more prominent than another type. To assist them, initial feedback was given to help them calibrate respective mouse click activity and reduce noise. The objective was to have change similar change in the magnitude of EMG at the time of mouse click.

Figure 2.3: *'Training'* phase; Participants were asked to perform respective mouse clicks on the blue buttons as the text written on them; A. Participant in going to perform 'LEFT' click on mouse; B. Participant in going to perform 'RIGHT' click on mouse.

Once the participant got familiar with the setup, the *'training'* phase would begin, during which the participant was asked to perform 25 left clicks and 25 right clicks. For each clicking task, a virtual button would appear on a random position at the screen, with 'LEFT' or 'RIGHT' randomly appearing inside the button, (see Figure 2.2). The participant would need to move the mouse pointer to the target position, then click either the left or right mouse button as accordingly. The movement of the mouse pointer in the protocol was used to mimic real-world scenarios to ensure the likelihood of muscle activation while moving. This enables false muscle activations to be included in model training due to mouse movements. After the click, the button disappeared, and the next random button appeared on the screen after two seconds. At the end of the session, the sEMG signals and the corresponding mouse click events (timing) were saved, with which a participant-specific model was trained by leave one out cross-validation procedure. Once the

model was trained, the third phase, namely *'real-time running'*, would start. The developed model was used in real-time to detect and register clicks and provide feedback to the participant in real-time.

2.4 Data Labeling

The following procedure segmented the acquired data, as shown in Figure 2.3. The timestamp of each mechanical down click (MC-Down) of the mouse button was used as the reference point (as time 0 in the subsequent description), with which four sections for each click were identified. First, between -200 ms and 0 ms is called the Training Window (TW), *i.e.* a 200 ms window before the MC-Down. The TW was used to extract the features of the two-click classes (LEFT and RIGHT). This part of the signal likely contained the EMG activity corresponding to muscular contraction onset just before the mechanical click along with the mouse movements. The Mechanical Click (MC) is the duration of the actual mouse click, in which the first sample of the

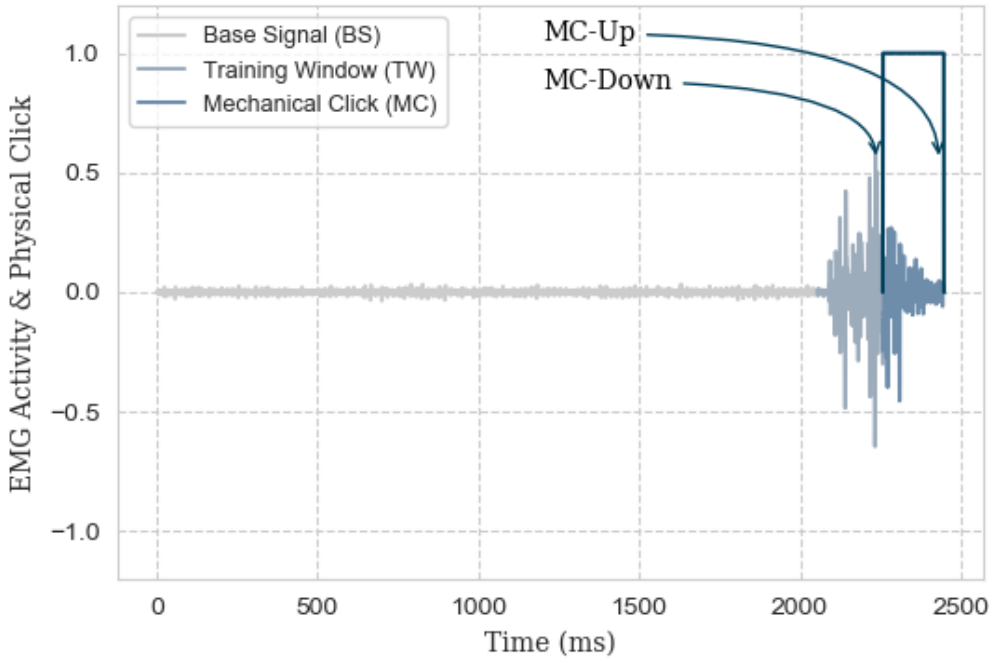

Figure 2.4: Various processing windows and corresponding EMG segments with respect to mechanical click. Base Signal (BS), two seconds of EMG activity as a result of mouse movement; Mechanical Click (MC), a mouse pressed duration of 240 ms; Training Window (TW), a window of 200 ms prior to MC-Down.

window down clicked, and the last sample was up clicked. The EMG activity of this period is excluded in training the model.

Third, Base Signal (BS) is all the EMG activities other than TW and MC. This part of the data contained participant's any muscle activities and background noise relating to his/her clicking intention, such as mouse pointer movements on the screen, subtle & unintentional muscle movements, and was used to extract features of the 'No-Click' class.

2.5 Data Segmentation

As a preliminary study, first (on first interossei) and third (on second interossei) channels were used in the detection of left and right clicks, respectively. The entire dataset was segmented into 25 segments for left-clicks and right-clicks separately from the respective channels. Each segment contained the data from the 25 mouse button clicks. Due to the smaller number of click trials, a leave-one-out validation procedure was used to evaluate system performance. For brevity, each data segment is subsequently referred to as a 'Click Unit'.

2.6 Click Detection as an Onset Detection Problem

The acquired EMG signals were initially processed using two onset detection methods previously reported in the literature: Teager-Kaiser Energy Operator (TKEO) and Root Mean Square (RMS) of window size of three samples. BS of all training 'Click Units' were used to determine the threshold for the detection onset. The two popular threshold criteria in sEMG onset detection are the *p* percentage of the BS's peak value and the mean plus *n* times the standard deviation of the BS, where the values of *p* and *n* should be tuned for each participant. In this study, we ranked all the peak values of the BS in the ascending order and used the mean of the top 100 peaks as the detection threshold for all participants. A previous study [10] reported that TKEO performed better than RMS in the presence of noise. The two methods were investigated on simulated data and experimental data by adding different levels of noise numerically, which resulted in the development of a novel method Divergence estimator (DE).

$$DE = \frac{1}{N}\sum_{n=1}^{N-1}(1-\alpha)\cdot|x_{(n)}| + \alpha\cdot\{|x_{(n)} - x_{(n+1)}| + |x_{(n)} - x_{(n-1)}|\} \qquad (16.16)$$

The above equation captures both magnitude and frequency related information of a signal, and α is a regularization parameter with 0.5 as its default value. For onset detection, the window size of three samples with a step size of one is used to make it consistent with TKEO and RMS. The detailed comparison of onset-detection performance among DE, TKEO, and RMS is shown in the Results section.

2.7 Click Detection as a Binary Classification Problem

For each participant in onset detection, the value of p and n needed to be tuned, and there was no single, one-size-fits-all method for TKEO, DE, and RMS. This motivated the investigation to try another approach using classification, which utilizes extracted features data points to develop the model that generalizes better for each participant. As such, the second detection approach investigated is to treat it as a binary classification program.

For the left click, three features RMS, DE, and TKEO, were extracted using the first channel using the window size of 1.5 ms (three samples). For longer window lengths, a window-based mean in TKEO's mathematical operation was added to make it fit for variable window sizes, which is call Extended (EXT)-TKEO. Here, EXT-TKEO serves as a feature in for subsequent classification. In each training 'Click Unit', the 'No-Click' class data points were extracted from BS, and the 'Click' class data points were extracted from TW. The step size of one was used and each data point was a 3x1 vector. Thereafter, the top 200 data points from both the classes ('Click' & 'No Click') were used to train the model using the Support Vector Machine (SVM) classification algorithm. The entire process was repeated for right-click using the third channel and a separate SVM model was generated. In the *real-time running* phase, these models were used simultaneously to detect both left and right clicks in real-time.

2.8 Performance Evaluation and System Behaviour

As detection latency was the main focus of the current study, sample-by-sample predictions were used. This led to redefine and consequently optimize confusion-matrix as per the objective of the study. A true-positive was registered when any sample of TW or MC was predicted as the 'Click' class by the algorithm, refer to Figure 2.4. If the click detection occurs in TW, a down-click was simulated by the algorithm, and the detection lead was calculated from the MC-Down. If the click detection occurs in MC, a delay was calculated from MC-Down. A false-positive was registered when any BS sample was predicted as a 'Click' by the algorithm. A false-negative was registered when there was a 'No-Click' prediction in TW or MC. A true-negative was registered when there was a 'No-Click' prediction in BS. Overall, two confusion-matrix were used separately for left, and right-click detection.

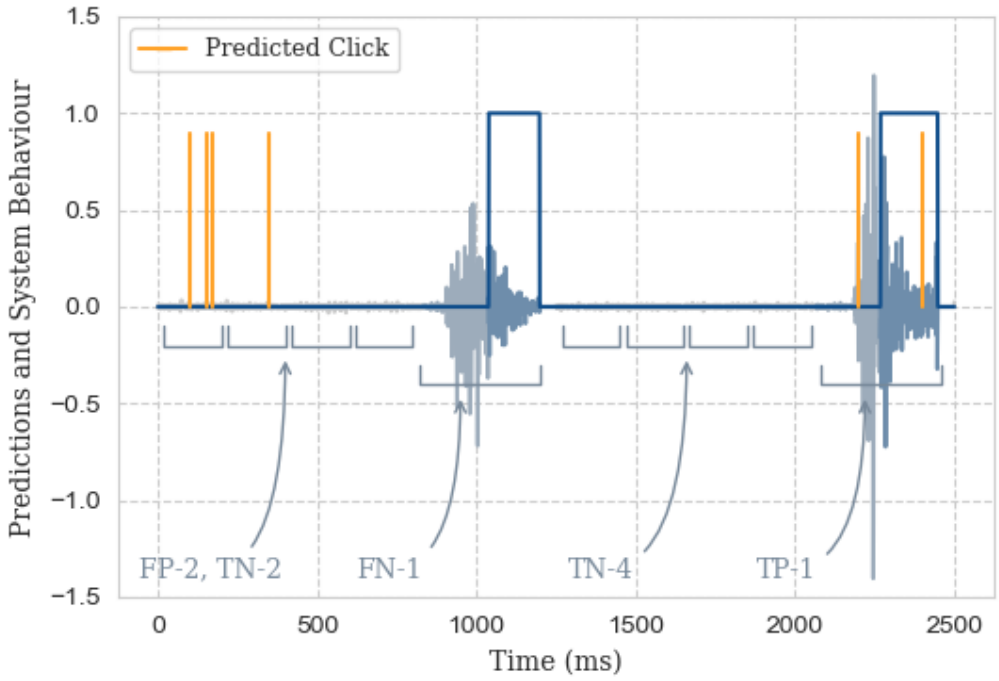

Figure 2.5: Revised confusion matrix example. First click has two false-positives, two true-negatives and one false-negative. Second click has four true-negatives and one true-positive.

A higher number of 'No-Click' class data points would give an unrealistic high value of accuracy (imbalanced dataset) if used as a performance metric. It gives equal weights to all four

categories; true-positives, true-negatives, false-positives, and false-negatives. Therefore, the F1-score [1], which is the harmonic mean of *precision* and *recall*, was used as a primary metric. A high value of *precision* ensures lower false detections and a high value of *recall* ensures no detection is missed. Therefore, for this study F1 score was chosen as a primary metric that represents method's true click detection performance. Furthermore, total clicks detected ahead from MC-Down, average lead time in milliseconds, and the effect of increasing window sizes are shown in Results for both left and right clicks.

2.9 EMG Simulation Test for Divergence Estimator (DE)

EMG signal numerical simulation can be as a straightforward process as stochastic Gaussian noise [49]. Other more advanced methods, such as simulating EMG as the summation of concurrently active motor unit action potential trains (MUAP), are also used in various research studies, when EMG is used to infer certain physiological parameters, such as conduction velocity and motor unit synchrony [50]. In this study, the simpler simulation approaches *i.e.* colored Gaussian noise were used. To investigate the onset-detection performance of various algorithms, different types of artifacts were used to contaminate the simulated EMG. Two types of noise, spiking (due to instrumentation) noise and motion artifact, were simulated. For each type of artifact, a total of 18 sets of simulated signals with six different signal-to-noise (SNR) ratio (2, 4, 6, 8, 10, and 12 dB) and three different sampling frequencies (1024, 2048, and 4096 Hz) were used to evaluate the detection performance. Each set consisted of 50 iterations of simulated EMG.

Ten seconds of simulated EMG were used in a sample-by-sample classification setting for low detection latency. First, five seconds were regarded as the reference signal and used to determine the detection threshold; the next five seconds were regarded as muscle activity signal. After applying onset-detection algorithms, the threshold for all was chosen as 80% of the reference signal's maximum amplitude. Detection was made when any sample crossed that threshold. For spiking noise, five noise artifacts were added to the reference signal. Each spike's amplitude was randomly chosen between zero to thirty percent of the maximum amplitude of the whole signal. For motion artifact, one simulated low-frequency (1 to 50 Hz) random signal of duration one to three seconds was added in the reference signal. The performance of TKEO & DE and RMS &

DE were compared and reported in the results section for spiking noise and motion artifact, respectively.

2.10 Statistical Analysis

The significance analysis was performed between onset methods and classification results. F1-scores for both left and right-click predictions were obtained using cross-validation for all twenty participants. First, the Shapiro–Wilk test was performed to test the normality of the F1-scores for both left and right-click. For right-click, all the methods (TKEO, RMS, DE, and Classification) were normally distributed, which moved analysis towards the parametric one-way ANOVA test, followed by posthoc multiple comparisons, if the significance of the main effect is detected. However, for left click, RMS and DE were not normally distributed, which led analysis towards the non-parametric Kruskal Wallis test, followed by individual method comparison using the Wilcoxon signed-rank test. The significance level of 0.05 ($p<0.05$) was used in all the tests. The entire statistical analysis was performed using the SciPy package.

Chapter 3

Results

This chapter explains the results and performances of Divergence Estimator (DE), click detection methods, and the effect of bigger window sizes.

3.1 EMG Simulation Results for Divergence Estimator (DE)

For simulated EMG, the performance of divergence estimator (DE) with different values α of were compared with TKEO and RMS in different noise conditions. The results of the algorithm's performance in spiking noise and motion artifacts are shown in Figures 3.1 and 3.2 respectively.

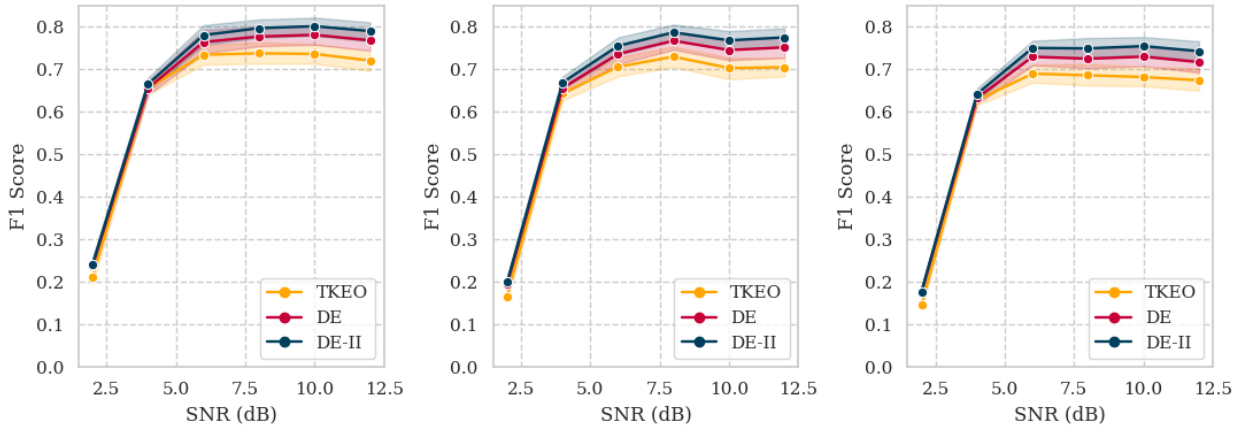

Figure 3.1: Detection performance in the presence of simulated spiking noise. A. Sampling Rate (1024 Hz); B. Sampling Rate (2048 Hz); C. Sampling Rate (4096 Hz); Mean F1 Score as a function of signal to noise ratio (SNR) of 50 iterations ($p < 0.05$). DE (α = 0.5) and DE-II (α = 0.8). The shaded area indicate the respective standard deviation in each case.

The performance of TKEO and DE in spiking noise is shown in Figure 3.1. In the simulation, the value of α was fixed to 0.5 for DE and 0.8 for DE-II. Both DE-II performed better DE followed by TKEO in case of spiking noise ($p < 0.05$). For the SNR of two decibels and 1024 Hz sampling rate, the F1 scores of DE-II and TKEO were around 0.24 and 0.21, which was improved to 0.79 and 0.72 for 12 dB SNR, respectively. Similar behavior was observed in other configurations with the sampling rate of 2048 Hz and 4096 Hz.

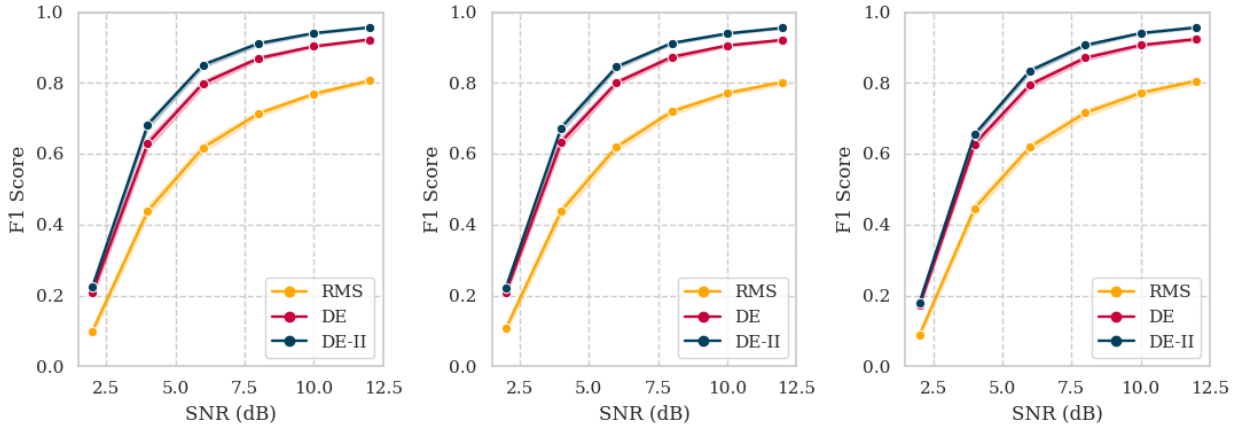

Figure 3.2: Detection performance in the presence of simulated motion artifacts. A. Sampling Rate (1024 Hz); B. Sampling Rate (2048 Hz); C. Sampling Rate (4096 Hz); Mean F1 Score as a function of signal to noise ratio (SNR) of 50 iterations ($p < 0.05$). DE ($\alpha = 0.5$) and DE-II ($\alpha = 0.75$). The shaded area indicate the respective standard deviation in each case.

For motion artifact, see Figure 3.2. The performance of RMS and DE are reported with two values of α as 0.5 and 0.75. The results confirmed the poor onset-detection performance of RMS in the case of motion artifacts which was suggested by the authors of [30].

Similar to spiking noise, DE-II performed better than DE followed by RMS in case of motion artifacts ($p < 0.05$). For the SNR of two decibels and 1024 Hz sampling rate, the F1 scores of DE-II and RMS were around 0.2 and 0.1, which got improved to 0.95 and 0.81 for 12 dB SNR, respectively. RMS performed the same in the other two configurations of 2048 Hz and 4096 Hz sampling rates.

3.2 Experimental EMG Data Results for Divergence Estimator (DE)

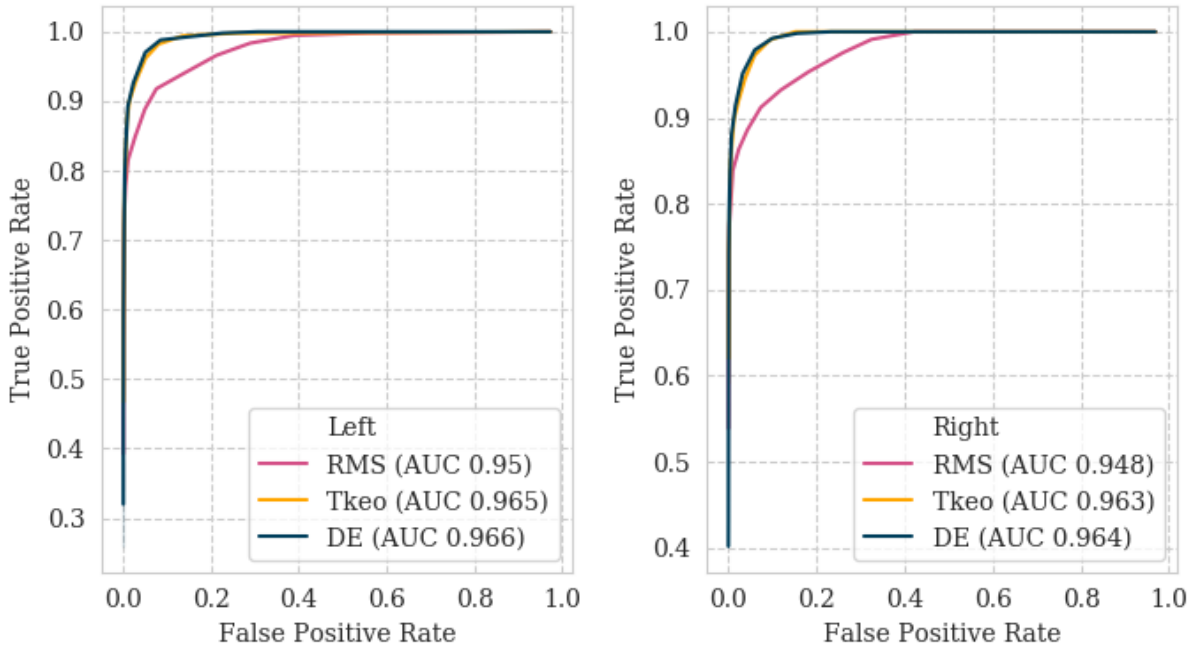

Figure 3.3: Mean ROC curve of TKEO, DE (α = 0.5) and RMS of all twenty participants for left and right click detections.

For experimental sEMG data, the onset detection performance of all algorithms was compared using acquired sEMG data of twenty participants with multiple thresholds. The mean ROC (Receiver Operating Characteristics) and AUC (Area Under the Curve) of DE (α = 0.5), RMS, and TKEO are reported in Figure 3.3. On average, for onset detection of both left and right clicks, the AUC of DE (α = 0.5) and TKEO were higher than that of RMS (0.96 and 0.96 vs 0.95). The ROC of DE (α = 0.5) and TKEO are highly similar.

3.3 Mouse Click Detection Results

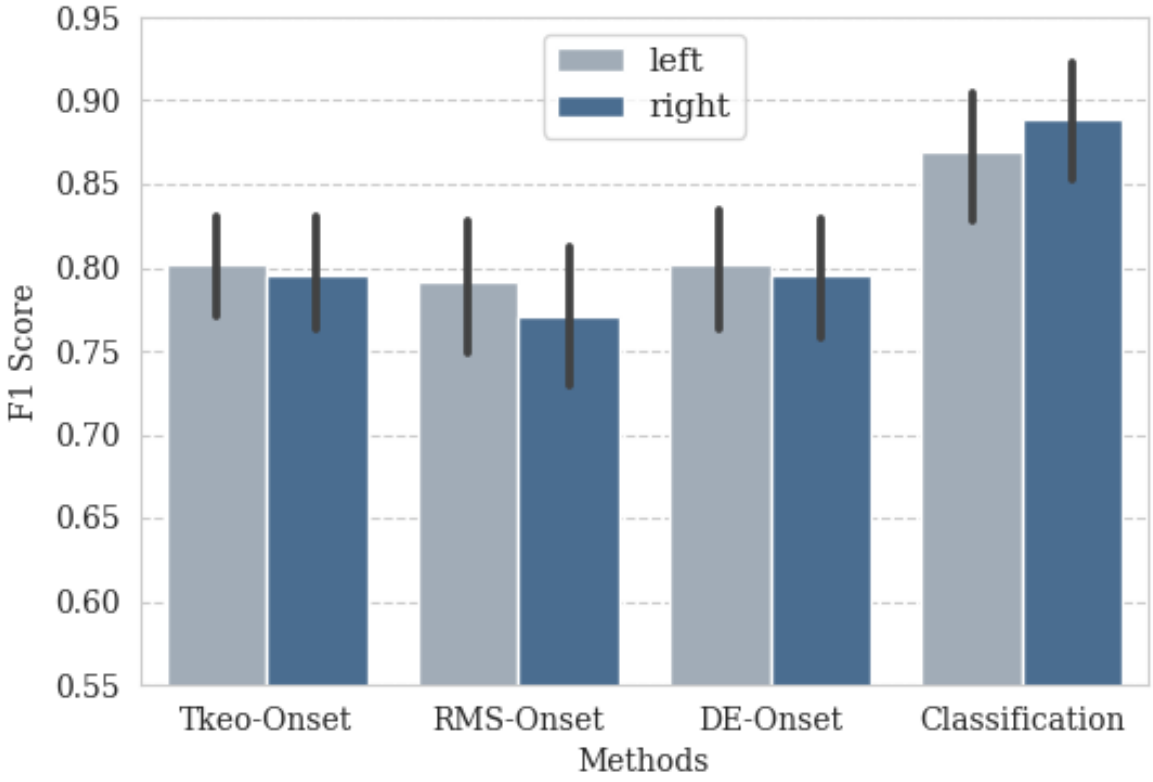

Figure 3.4: Detection performance comparison between onset detection and binary classification methods for left and right mouse click detection.

The performance comparison between binary classification and onsets detection methods for left and right click using 1.5 ms window size is shown in Figure 3.4. For the left click detection, the F1 score of binary classification was 0.86 ± 0.09 which was significantly higher ($p < 0.001$) than RMS (0.78 ± 0.09), DE (0.79 ± 0.08) and TKEO (0.79 ± 0.07). Likewise, the binary classification performance for right click (0.88 ± 0.08) was significantly higher ($p<0.01$) than DE (0.79 ± 0.08), TKEO (0.79 ± 0.08) and RMS (0.76 ± 0.10).

Table 3.2 'Left' click detection results (F1-scores) of all participants based on leave one out validation.

Participants	TKEO	DE	RMS	Binary Classification
P-01	0.87	**0.89**	0.87	**0.90**
P-02	0.72	**0.73**	0.70	**0.76**
P-03	0.82	**0.81**	0.85	**0.87**
P-04	0.74	**0.68**	0.75	**0.82**
P-05	0.84	**0.84**	0.81	**0.96**
P-06	0.85	**0.85**	0.87	**0.94**
P-07	0.67	**0.69**	0.64	**0.96**
P-08	0.80	**0.83**	0.79	**0.84**
P-09	0.59	**0.56**	0.51	**0.60**
P-10	0.84	**0.84**	0.86	**0.84**
P-11	0.76	**0.79**	0.75	**0.97**
P-12	0.74	**0.72**	0.71	**0.71**
P-13	0.83	**0.83**	0.83	**0.83**
P-14	0.79	**0.79**	0.79	**0.81**
P-15	0.90	**0.90**	0.90	**0.92**
P-16	0.87	**0.88**	0.88	**0.89**
P-17	0.82	**0.82**	0.8	**0.94**
P-18	0.82	**0.83**	0.83	**0.86**
P-19	0.86	**0.86**	0.85	**1**
P-20	0.79	**0.79**	0.75	**0.88**
Average	0.79	**0.79**	0.78	**0.86**

Table 3.2 'Right' click detection results (F1-scores) of all participants based on leave one out validation.

Participants	TKEO	DE	RMS	Binary Classification
P-01	0.79	**0.84**	0.82	**0.81**
P-02	0.81	**0.76**	0.81	**0.98**
P-03	0.89	**0.84**	0.86	**0.95**
P-04	0.84	**0.83**	0.83	**0.86**
P-05	0.75	**0.67**	0.73	**0.85**
P-06	0.77	**0.68**	0.76	**0.97**
P-07	0.75	**0.78**	0.75	**0.96**
P-08	0.82	**0.77**	0.83	**0.82**
P-09	0.83	**0.82**	0.86	**0.87**
P-10	0.74	**0.63**	0.74	**0.83**
P-11	0.68	**0.58**	0.63	**0.88**
P-12	0.86	**0.83**	0.84	**0.92**
P-13	0.74	**0.81**	0.73	**0.84**
P-14	0.79	**0.77**	0.80	**0.72**
P-15	0.90	**0.90**	0.89	**1**
P-16	0.66	**0.67**	0.67	**0.83**
P-17	0.64	**0.62**	0.67	**0.74**
P-18	0.83	**0.86**	0.84	**0.96**
P-19	0.96	**0.96**	0.96	**0.91**
P-20	0.76	**0.68**	0.77	**1**
Average	0.79	**0.79**	0.76	**0.88**

3.4 Effect of bigger window sizes for binary classification

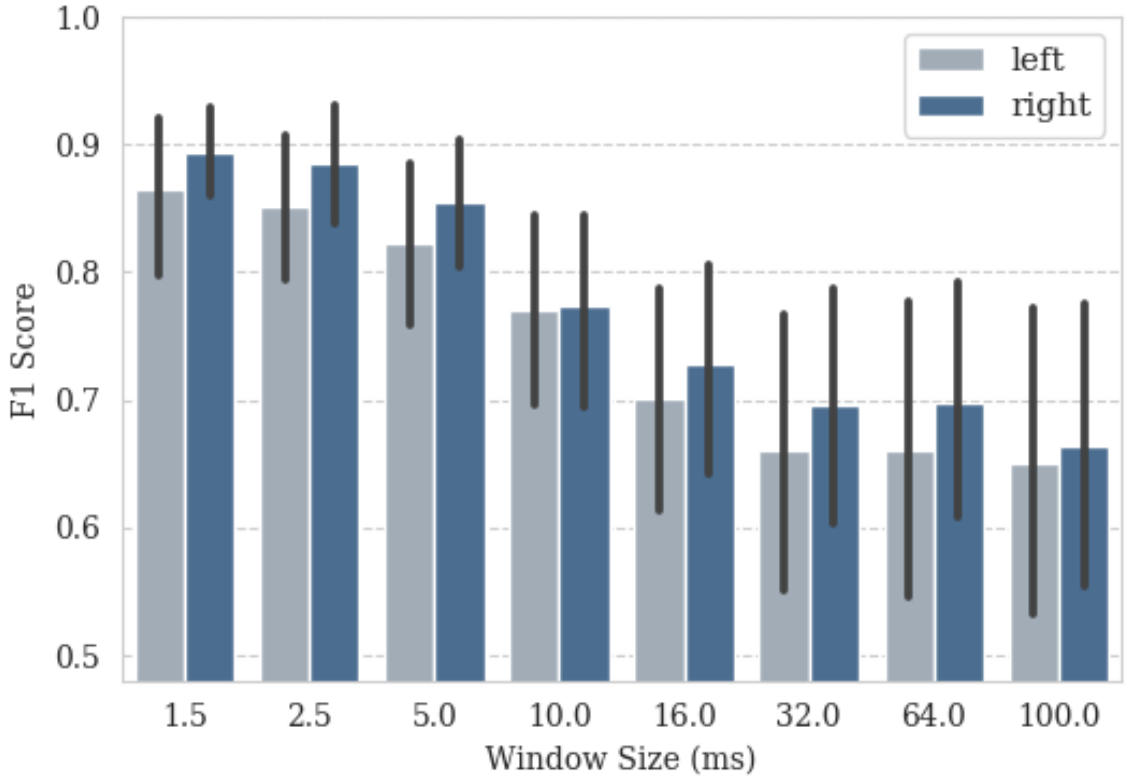

Figure 3.5: Effect of increasing window size in binary classification performance for left and right click detection.

Figure 3.5 shows the effect of increasing window size in binary classification. Performances were tested in a 1.5 ms to 100 ms window size setting. For both the clicks, the detection performance decreased with the increase in window size. From window sizes 1.5 ms to 100 ms, the F1 score dropped from 0.85 to 0.64 and 0.88 to 0.66 for left and right-click, respectively. In addition to the detection performance, click with leads or average click detections before MC-Down were also reduced, see Figure 3.6 A, from 20 ± 3 to 8 ± 3 for left click and from 20 ± 2 to 9 ± 2 right-click as a function of increasing the window size.

3.5 Timing Estimates

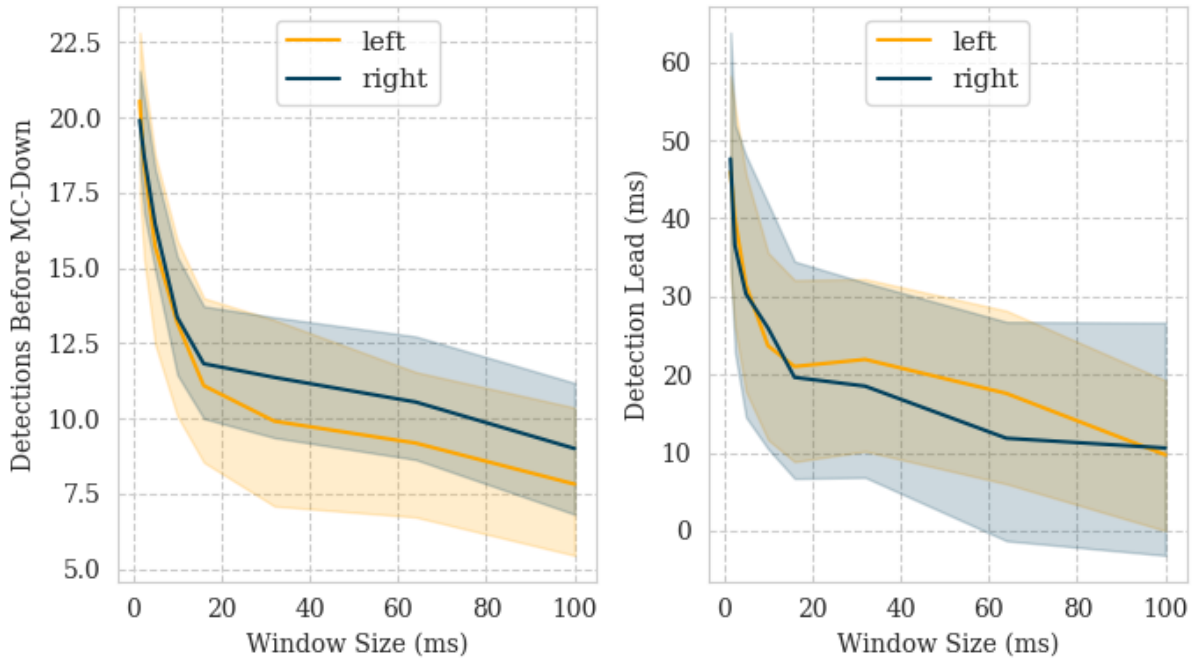

Figure 3.6: A. Average detected clicks before MC-Down for all participants as a function of increasing window size; B. Average detection lead for all participants as a function of increasing window size.

The performance of binary classification for different window sizes is reported in Figure 3. Figure 3.6 B shows the behavior of average detection lead with respect to increasing window size. It states the negative correlation between detection lead and window size. It dropped from 45 milliseconds to 10 milliseconds for a window size of 1.5 milliseconds and 100 milliseconds, respectively. Figure 3.5, 3.6 A, 3.6 B shows the performance and detection lead drop till 40 milliseconds window size was greater than the rest of the window sizes.

Figure 3.4 shows, for mouse click reaction improvement (or higher detection leads), the binary classification using SVM with our proposed features outperformed existed onset detection methods. Figure 3.6 B shows, the best performance of this study was achieved at the window size of 1.5 milliseconds, the average detection lead was approximately 45 milliseconds, for both ‘LEFT’ and ‘RIGHT’ clicks. Figure 3.5 shows, for the same window size (1.5 milliseconds), the F1-score performed the best, 0.85 for the ‘LEFT’ click and 0.88 for the ‘RIGHT’ click.

Chapter 4

Discussion

At the present, pattern recognition based machine learning in EMG is limited to academic and research applications. HMI applications with electrophysiological signals are applied in rehabilitation, meditation, heart-rate monitoring using EMG, EEG, and, ECG respectively. Beyond these applications, HMI has yet to find broader applications in everyday life. This study focused on improving the close-loop control (or feedback) delay of HMI's based on surface EMG, which can be used in various time-critical applications, such as VR/AR, and on-demand exoskeletons.

4.1 Divergence Estimator (DE)

In this study, a novel method, namely divergence estimator (DE), was proposed for the onset detection of sEMG in the context of ultra-short latency (a few milliseconds). This new feature extraction method was compared with the other two commonly used sEMG onset detection features, TKEO, and RMS. DE was tested with threshold-based techniques as well as pattern recognition techniques.

Few studies have previously investigated the low latency context of EMG analysis [22, 51]. Both the studies considered low latency as an onset detection problem. In [51], the authors used a window size of 32 milliseconds with 4 milliseconds overlap and tested their proposed method in the presence of spiking noise. Their method outperformed TKEO for window sizes of a few hundred milliseconds. However, they did not consider the detection latency of a few milliseconds which exists in problems like mouse click detection. In another study, the author proposed a new onset detection method for low latency detection, but there is no comparison between their proposed method and existing common EMG onset detection algorithms [22].

Different types of noise (spiking and motion artifact) in acquired experimental data motivated the development of DE. The intuition was to operate with the same onset-detection method in different noise scenarios. For simulated data, Figures 3.1 and 3.2 showed TKEO performed poorly in spiking noise, and RMS performed poorly in motion artifacts. The tests

conducted in different noise scenarios and different values of α in simulated EMG confirmed the utility α in DE's performance, refer to Figures 3.1 and 3.2. The parameter α in DE is a key feature and can be tuned according to the dataset to improve EMG onset-detection performance. For experimental data (n = 20), the mean ROC and AUC of TKEO, RMS, and DE were computed. The DE (α = 0.5) outperformed RMS but the performance was similar to TKEO. However, the value of α was fixed to 0.5 for ROC calculation which can be optimized to outperform TKEO for onset detection. In addition, just like RMS, DE can also be employed as a feature in pattern recognition techniques. Section 2.7 described its usage as a feature, along with extended-TKEO and RMS. Collectively all three outperformed for mouse click detection and reducing detection-latency.

4.2 Binary Classification for click detection

Figure 3.4 shows, for mouse click detection, binary classification using SVM outperformed remaining popular onset detection methods. A previous study considered low latency as an onset detection problem [22]. This motivated the preliminary investigation of mouse click detections started through TKEO and RMS onset-detection methods, which suggested that both strategies were not one-size-fits-all. This encouraged us to look for alternative methods that led to the development of DE. The goal was to deal with various forms of noise with just one technique.

Although the DE can be tuned to optimum performance for onset-detection, the key drawback of the rule-based threshold system is that various types of noise are not taken into account for calculation. This limits the optimum performance of click detection. In comparison, approaches focused on pattern recognition use information that exists in acquired data to extract the best hyperplane to classify the data points. This behavior can be observed in figure 3.4 where all initial approaches are outperformed by binary classification using SVM.

Figure 3.6 indicates the detrimental effect of the greater window size. This is due to the fact the detections are made so delayed they were counted as false negative for mouse click detection. This effect restricted us to the study of wider window size and frequency domain characteristics. Our investigation led us to use our proposed features; DE, Extended-TKEO, and RMS. Also, features were sorted in decreasing order instead of using data points directly from the extracted features, followed by the selection of the top two hundred data points from each class. This ensures low false positives in the detection of mouse clicks and higher true click detections before physical mouse clicks.

Traditionally, EMG based pattern recognition uses window sizes of up to a few hundred milliseconds [23], allowing frequency domain features the privilege of extracting. Capturing low-latency detection up to a few milliseconds sounds unreasonable for bigger window sizes. It is difficult to catch the frequency domain features in a window size of a few milliseconds (less than five ms), which restricts our analysis to the usage of time-domain features only. Moreover, typical EMG time-domain features, such as waveform length, zero-crossing, or more, refer to section

1.2.3, are inadequate for limited window sizes to obtain any useful information. The maximum and minimum values of zero-crossings for a window size of 1.5 ms (sampling rate 2048 Hz) were two and zero, which doesn't contribute much to the classification.

Another significant difference in the analysis approach is the step-size of one, over window overlaps. Every data point needs to be analyzed as soon as it is collected from the hardware to ensure the earliest detection. The processing delay was introduced by window-overlaps, which was a significant bottleneck for the objective of this study. While sample by sample processing introduced additional overhead to system output, the low-level programming language C/C++ was used to tackle this problem.

4.3 Detection Leads

The results of Figure 3.4, showed that the proposed DE, combined with the binary classification approach, outperformed all other combinations of feature extraction methods and threshold detection or classification. For both click detection and detection lead, the best performance was obtained at 1.5-millisecond window size. Across all twenty participants, the detection lead was approximately 45 milliseconds and the detection performance (F1-score) for left and right mouse click detection were 0.87 and 0.88, respectively. Better performance of classification was due to data-driven policy compared to onset detection, which relies on the rule-based system for threshold selection. It was also examined that the classic sEMG time-domain features proposed in [23], which is the most popular sEMG feature extraction method, performed particularly poorly in the context of ultra-short latency. This is because features such as zero-crossing and slope-sign change are considered non stationary [52] for very short window sizes of few milliseconds.

Figure 3.6 shows the seemingly unintuitive deteriorating performance with the increasing window size. In the experimental protocol, the duration of mouse-clicks (between MC-Down and

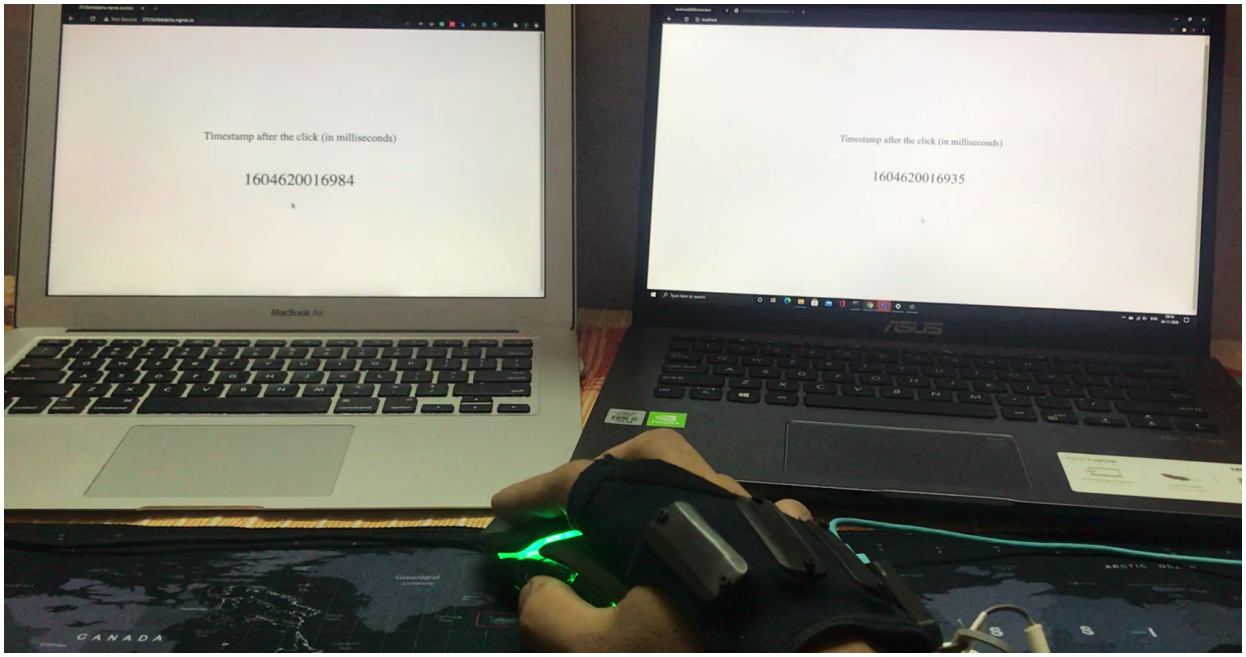

Figure 4.1: A detection lead example. The system on the 'Right' is connected to sEMG based glove and system on the 'Left' is connected to gaming mouse. After a mouse click, the click time recorded by the 'Right'system was 49 ms earlier than 'Left' system.

MC-Up) was very short (typically < 150 ms), simulating realistic mouse clicks. As such, a true-positive can only be registered within this short period. This presented a serious challenge for longer processing windows. The longer the windows, the more likely detections would occur outside the mouse-click duration, hence considered as false detection. If this 'window of opportunity' was to be relaxed, higher detection accuracy might be obtained. However, it would defeat the purpose of the current study: ultra-short latency detection (or even prediction).

The proposed method was tested in the 'real-time running' phase to validate the click reaction time improvements. A script was written to display Unix Epoch time in milliseconds when clicked on the screen, which was deployed into two systems. An example of detection lead is shown in Figure 4.1. After the 'calibration' and 'training' phase, the left system was connected to a mechanical mouse and the right system to the EMG glove. When the participant pressed the mouse click, the timestamp recorded after clicks are shown in Figure 4.1 for both the systems. For a real-time test, the mean and standard deviation of the detection lead was 55 ± 23 milliseconds (n = 20 clicks). Further details about reaction time lead and detection performance are reported in the results section.

4.4 Limitations and Future Work of the Study

The two key research limitations are. First, to distinguish the 'LEFT' and 'RIGHT' mouse clicks, only three electrodes were used. And even though sEMG from three channels were acquired in the experiment setup, the results from the other two channels were not reported here due to poorer performance. For electrode placement, muscles closer to the respective fingers were selected. While the results of the click detection acceptable, to identify the best location of electrodes, a high-density electrode grid should be used. We found that spatial domain features utilizing three electrodes did not contribute much to pattern recognition performance when conducting experiments. The other drawback was the set of glove size that could not be modified according to the hand size of the person. This led to incorrect positioning of electrodes for some participants on their respective muscles, hence the signal-to-noise ratio (SNR) was not good therefore leading to lower performance.

For future work, although the proposed pattern recognition method is tested in a binary classification setting, it is interesting to see the performance of the system in a multi-class problem setting. On the hardware aspect, a high-density EMG grid needed to be used to identify the optimal electrode placement on muscle and acquire spatial domain features for improved performance. Not only can a high-density electrode grid increase the efficiency of the click detection, but it can also boost the reaction lead for mouse clicks. In addition, the glove with movable electrodes in the glove or multiple gloves that could accommodate different hand sizes would perform better. On the algorithms aspect, methods using deep learning (LSTMs and GRUs) are getting popular in surface EMG studies [53]. The development in deep leaning based time-series prediction can be explored low-latency context.

Chapter 5

Conclusion

This study primarily focused on three analysis. First, the evaluation of the proposed novel method Divergence Estimator under various noise settings and its comparison with existing onset-detection techniques. The performance results of DE were reported for both simulation and experimental data, which states that DE either outperformed or similar to exiting methods like TKEO and RMS. Second, the detection of mouse click detection existing EMG onset-detection methods and binary classifications. Results showed binary classification outperformed the remaining onset detection methods used in the analysis. Third, the effect of different processing window size on detection latency. The results showed that mean detection leads to 45 milliseconds were achieved across all participants for a very small window size (1.5 milliseconds).

For onset-detection the performance of TKEO and DE are similar and both outperformed RMS. Although the value of alpha in DE was designed to be optimized for each dataset, for demonstration purposes, a constant value of alpha (0.5) was used for DE in ROC - AUC and onset-detection calculations. Second, the approach using binary classification was found to be best suited for low-latency problems. Traditionally EMG pattern recognition doesn't perform well for smaller window sizes, but our proposed set of features DE, RMS, and Extended TKEO outperformed the existing onset-detection techniques. Third, the experiments showed, for the optimized values of alpha the performance of DE was superior compared to TKEO and RMS in spiking and motion artifact noise. The tests were conducted on various SNR ratios and multiple iterations.

This study was focused to investigate the possibility of improving user's reaction time using EMG-based HMI for desktop mouse click and the results of the study confirmed the likelihood of the same. In conclusion, achieving low-latency HMI using sEMG and pattern recognition with extremely small window sizes are possible, which can be used in many time-critical applications, including human-robotic interaction and VR/AR applications.

References

[1] M. Valenzuela and B. Bordoni, "Anatomy, shoulder and upper limb, hand palmar interosseous muscle," 2019.

[2] K. Dawson-Amoah and M. Varacallo, "Anatomy, Shoulder and Upper Limb, Hand Intrinsic Muscles," in *StatPearls [Internet]*: StatPearls Publishing, 2019.

[3] L. Van Dijk, C. K. Van Der Sluis, H. W. Van Dijk, and R. M. Bongers, "Learning an EMG controlled game: Task-specific adaptations and transfer," *PloS one,* vol. 11, no. 8, p. e0160817, 2016.

[4] J. Cannan and H. Hu, "Human-machine interaction (HMI): A survey," *University of Essex,* 2011.

[5] J. K. Suhr, H. G. Jung, K. Bae, and J. Kim, "Automatic free parking space detection by using motion stereo-based 3D reconstruction," *Machine Vision and Applications,* vol. 21, no. 2, pp. 163-176, 2010.

[6] P. Jia and H. Hu, "Active shape model-based user identification for an intelligent wheelchair," *International Journal of Advanced Mechatronic Systems,* vol. 1, no. 4, pp. 299-307, 2009.

[7] I. S. MacKenzie, "An eye on input: research challenges in using the eye for computer input control," in *Proceedings of the 2010 Symposium on Eye-Tracking Research & Applications*, 2010, pp. 11-12.

[8] D. Arsic, B. Hornler, B. Schuller, and G. Rigoll, "A hierarchical approach for visual suspicious behavior detection in aircrafts," in *2009 16th International Conference on Digital Signal Processing*, 2009: IEEE, pp. 1-7.

[9] A. Gárate, N. Herrasti, and A. López, "GENIO: an ambient intelligence application in home automation and entertainment environment," in *Proceedings of the 2005 joint conference on Smart objects and ambient intelligence: innovative context-aware services: usages and technologies*, 2005, pp. 241-245.

[10] I. Tashev, M. Seltzer, Y.-C. Ju, Y.-Y. Wang, and A. Acero, "Commute UX: Voice enabled in-car infotainment system," 2009.

[11] N. Miller, O. C. Jenkins, M. Kallmann, and M. J. Mataric, "Motion capture from inertial sensing for untethered humanoid teleoperation," in *4th IEEE/RAS International Conference on Humanoid Robots, 2004.*, 2004, vol. 2: IEEE, pp. 547-565.

[12] S. Donati, V. Annovazzi-Lodi, L. Bottazzi, and D. Zambarbieri, "Pickup of head movement in vestibular reflex experiments with an optical fiber gyroscope," *IEEE Journal of Selected Topics in Quantum Electronics,* vol. 2, no. 4, pp. 890-893, 1996.

[13] S. Rönnbäck, J. Piekkari, K. Hyyppä, T. Berglund, and S. Koskinen, "A semi-autonomous wheelchair towards user-centered design," in *International Conference on Computers for Handicapped Persons*, 2006: Springer, pp. 701-708.

[14] H. Kawamoto and Y. Sankai, "Power assist system HAL-3 for gait disorder person," in *International Conference on Computers for Handicapped Persons*, 2002: Springer, pp. 196-203.

[15] J.-U. Chu, I. Moon, and M.-S. Mun, "A real-time EMG pattern recognition based on linear-nonlinear feature projection for multifunction myoelectric hand," in *9th International Conference on Rehabilitation Robotics, 2005. ICORR 2005.*, 2005: IEEE, pp. 295-298.

[16] E. Costanza, A. Perdomo, S. A. Inverso, and R. Allen, "EMG as a subtle input interface for mobile computing," in *International Conference on Mobile Human-Computer Interaction*, 2004: Springer, pp. 426-430.

[17] A. Pradhan, N. Jiang, V. Chester, and U. Kuruganti, "Linear regression with frequency division technique for robust simultaneous and proportional myoelectric control during medium and high contraction-level variation," *Biomedical Signal Processing and Control,* vol. 61, p. 101984, 2020.

[18] A. Bardack *et al.*, "EMG Biofeedback Videogame System for the Gait Rehabilitation of Hemiparetic Individuals," 2010.
[19] E. L. Schuurink, J. Houtkamp, and A. Toet, "Engagement and EMG in serious gaming: Experimenting with sound and dynamics in the Levee Patroller training game," in *International Conference on Fun and Games*, 2008: Springer, pp. 139-149.
[20] S. Melnyk, K. Alam, A. G. Tesfay, and H. D. Schotten, "Hybrid MAC for Low Latency Wireless Communication Enabling Industrial HMI Applications," in *2018 IEEE 4th International Symposium on Wireless Systems within the International Conferences on Intelligent Data Acquisition and Advanced Computing Systems (IDAACS-SWS)*, 2018: IEEE, pp. 21-24.
[21] informatica.com. "What is Ultra Low Latency?" https://www.informatica.com/in/services-and-training/glossary-of-terms/ultra-low-latency-definition.html (accessed.
[22] A. Kontunen *et al.*, "Low-latency EMG Onset and Termination Detection for Facial Pacing," in *EMBEC & NBC 2017*: Springer, 2017, pp. 1016-1019.
[23] K. Englehart and B. Hudgins, "A robust, real-time control scheme for multifunction myoelectric control," *IEEE transactions on biomedical engineering,* vol. 50, no. 7, pp. 848-854, 2003.
[24] F. Buchthal and H. Schmalbruch, "Motor unit of mammalian muscle," *Physiological reviews,* vol. 60, no. 1, pp. 90-142, 1980.
[25] P. C. Doerschuk, D. E. Gustafon, and A. S. Willsky, "Upper extremity limb function discrimination using EMG signal analysis," *IEEE Transactions on Biomedical Engineering,* no. 1, pp. 18-29, 1983.
[26] E. A. Clancy, E. L. Morin, and R. Merletti, "Sampling, noise-reduction and amplitude estimation issues in surface electromyography," *Journal of electromyography and kinesiology,* vol. 12, no. 1, pp. 1-16, 2002.
[27] B. Gerdle, S. Karlsson, S. Day, and M. Djupsjöbacka, "Acquisition, processing and analysis of the surface electromyogram," in *Modern techniques in neuroscience research*: Springer, 1999, pp. 705-755.
[28] P. W. Hodges and B. H. Bui, "A comparison of computer-based methods for the determination of onset of muscle contraction using electromyography," *Electroencephalography and clinical Neurophysiology,* vol. 101, no. 6, pp. 511-519, 1996.
[29] J. F. Kaiser, "On a simple algorithm to calculate the'energy'of a signal," in *International conference on acoustics, speech, and signal processing*, 1990: IEEE, pp. 381-384.
[30] S. P. Y. Jane and S. Sasidhar, "Sign Language Interpreter: Classification of Forearm EMG and IMU Signals for Signing Exact English," in *2018 IEEE 14th International Conference on Control and Automation (ICCA)*, 2018: IEEE, pp. 947-952.
[31] S. Solnik, P. Rider, K. Steinweg, P. DeVita, and T. Hortobágyi, "Teager–Kaiser energy operator signal conditioning improves EMG onset detection," *European journal of applied physiology,* vol. 110, no. 3, pp. 489-498, 2010.
[32] M. Tabie and E. A. Kirchner, "EMG onset detection-comparison of different methods for a movement prediction task based on EMG," in *International Conference on Bio-inspired Systems and Signal Processing*, 2013, vol. 2: SciTePress, pp. 242-247.
[33] S. Mukhopadhyay and G. Ray, "A new interpretation of nonlinear energy operator and its efficacy in spike detection," *IEEE Transactions on biomedical engineering,* vol. 45, no. 2, pp. 180-187, 1998.
[34] A. Phinyomark, C. Limsakul, and P. Phukpattaranont, "A novel feature extraction for robust EMG pattern recognition," *arXiv preprint arXiv:0912.3973,* 2009.
[35] P. V. Komi and P. Tesch, "EMG frequency spectrum, muscle structure, and fatigue during dynamic contractions in man," *European journal of applied physiology and occupational physiology,* vol. 42, no. 1, pp. 41-50, 1979.

[36] O. Paiss and G. F. Inbar, "Autoregressive modeling of surface EMG and its spectrum with application to fatigue," *IEEE transactions on biomedical engineering,* no. 10, pp. 761-770, 1987.
[37] R. J. Schwarz and C. Taylor, "The anatomy and mechanics of the human hand," *Artificial limbs,* vol. 2, no. 2, pp. 22-35, 1955.
[38] A. A. Adewuyi, L. J. Hargrove, and T. A. Kuiken, "An analysis of intrinsic and extrinsic hand muscle EMG for improved pattern recognition control," *IEEE Transactions on Neural Systems and Rehabilitation Engineering,* vol. 24, no. 4, pp. 485-494, 2015.
[39] R. L. Linscheid, K. N. An, and R. M. Gross, "Quantitative analysis of the intrinsic muscles of the hand," *Clinical Anatomy: The Official Journal of the American Association of Clinical Anatomists and the British Association of Clinical Anatomists,* vol. 4, no. 4, pp. 265-284, 1991.
[40] M. Zecca, S. Micera, M. C. Carrozza, and P. Dario, "Control of multifunctional prosthetic hands by processing the electromyographic signal," *Critical Reviews™ in Biomedical Engineering,* vol. 30, no. 4-6, 2002.
[41] K. Englehart, B. Hudgins, P. A. Parker, and M. Stevenson, "Classification of the myoelectric signal using time-frequency based representations," *Medical engineering & physics,* vol. 21, no. 6-7, pp. 431-438, 1999.
[42] M. A. Oskoei and H. Hu, "Myoelectric control systems—A survey," *Biomedical signal processing and control,* vol. 2, no. 4, pp. 275-294, 2007.
[43] E. Scheme and K. Englehart, "Electromyogram pattern recognition for control of powered upper-limb prostheses: state of the art and challenges for clinical use," *Journal of Rehabilitation Research & Development,* vol. 48, no. 6, 2011.
[44] Y. Guo, T. Hastie, and R. Tibshirani, "Regularized linear discriminant analysis and its application in microarrays," *Biostatistics,* vol. 8, no. 1, pp. 86-100, 2007.
[45] P. Geethanjali and K. Ray, "A low-cost real-time research platform for EMG pattern recognition-based prosthetic hand," *IEEE/ASME Transactions on mechatronics,* vol. 20, no. 4, pp. 1948-1955, 2014.
[46] I. Vujaklija *et al.*, "Translating research on myoelectric control into clinics—Are the performance assessment methods adequate?," *Frontiers in neurorobotics,* vol. 11, p. 7, 2017.
[47] J. M. Hahne, M. Markovic, and D. Farina, "User adaptation in myoelectric man-machine interfaces," *Scientific reports,* vol. 7, no. 1, pp. 1-10, 2017.
[48] N. Jiang, J. L. Vest-Nielsen, S. Muceli, and D. Farina, "EMG-based simultaneous and proportional estimation of wrist/hand kinematics in uni-lateral trans-radial amputees," *Journal of neuroengineering and rehabilitation,* vol. 9, no. 1, p. 42, 2012.
[49] C. J. De Luca, "Surface electromyography: Detection and recording," *DelSys Incorporated,* vol. 10, no. 2, pp. 1-10, 2002.
[50] D. Farina, A. Crosetti, and R. Merletti, "A model for the generation of synthetic intramuscular EMG signals to test decomposition algorithms," *IEEE transactions on biomedical engineering,* vol. 48, no. 1, pp. 66-77, 2001.
[51] X. Zhang and P. Zhou, "Sample entropy analysis of surface EMG for improved muscle activity onset detection against spurious background spikes," *Journal of Electromyography and Kinesiology,* vol. 22, no. 6, pp. 901-907, 2012.
[52] M. Bilodeau, M. Cincera, A. B. Arsenault, and D. Gravel, "Normality and Stationarity of EMG Signals of Elbow Flexor Muscles During Ramp and Step Isometric," *J. Electromyogr. Kinesiol,* vol. 7, no. 2, pp. 87-96, 1997.
[53] Y. Wu, B. Zheng, and Y. Zhao, "Dynamic gesture recognition based on LSTM-CNN," in *2018 Chinese Automation Congress (CAC)*, 2018: IEEE, pp. 2446-2450.